Journal of Theoretical and Applied Information Technology
15th November 2016. Vol.93. No.1

ISSN: 1992-8645 www.jatit.org E-ISSN: 1817-3195

ANALYSIS OF SYNTHETIC APERTURE RADAR IMAGES USING BRUTE FORCE THRESHOLDING AND GRADIENT GUIDE FILTERS

[1]M.L.M. LAKSHMI, [2] S.V.A.V. PRASAD, [3] MD. ZIA UR RAHMAN

[1]research Scholar, Department Of Ece, Lingaya's University, Faridabad, India.
[2] Department Of Ece, Lingaya's University, Faridabad, India.
[3]department Of Ece, Kkr & Ksr Inistitute Of Technology And Science, Vinjanampadu, Guntur-522017 Ap, India.
E-mail:[1]mlmlakshmi9@gmail.com, [2]prasad.svav@gmail.com, [3]mdzr55@gmail.com

ABSTRACT

Nowadays Imaging Radars (IR) finds many applications, in both civilian and defense fields to observe various scenarios over the horizon. Due to the rapid development of space borne and air borne platforms Synthetic Aperture Radars (SAR) becomes as an electronic eye to monitor different terrain features, various activities on the globe. As a result, analysis of SAR images is desirable to obtain high resolution electromagnetic (EM) images. In order to fulfill these requirements we propose a novel enhancement technique to de-speckle SAR images and to provide high resolution SAR images for the specific terrain monitoring. The proposed technique is a hybrid version of an improved brute force thresholding (BFT) based undecimated wavelet transform. The improved BFT combined with total variance process removes the speckle noise by preserving texture and edges. After this de-speckling process the image undergoes an enhancement process by gradient domain guided image filter (GDGIF). This GDGIF makes sharp enhancement and facilitates good quality SAR image for terrain analysis. GDGIF performs better than conventional guided image filter (GIF) and weighted guided filter (WGF). Simulation results confirm that the proposed realizations are well suited for real time applications. By comparing performance measures shown in Table II, the proposed method achieves better results in terms of minimum MD of 0.210, minimum MSE of 2.72E-04 and maximum PSNR of 35.658.

Keywords: *Electromagnetic Image, Image Enhancement, Imaging Radar, Speckle Noise, Synthetic Aperture.*

1. INTRODUCTION

Synthetic aperture radar (SAR) facilitates terrain imaging based on reflectivity of electromagnetic illumination from satellites. Because of this feature SAR becomes an important EM sensor in various remote sensing applications such as geo hazard investigation, earth environment monitoring, observing icebergs in sea, movement of various troops etc., with the capability of all time, all weather observation around the globe. To facilitate over the horizon observations SARs associated with synthesized antennas. In SAR imaging methodology, the entire terrain of interest is divided in to several imaginary patches. The SAR antenna illuminates these patches by changing its azimuth and elevation angles. The EM reflectivity from these patches are received back, combined and recorded by the SAR. This process is called as pulse integration. A coherent transmitter is used in SARs to ensure the pulse integration process in phase with all the received echoes. Due to the coherent transmitter and pulse integration process a noise called speckle noise come in to the picture. This speckle noise is multiplicative in nature. Normal enhancement techniques are not able to de-speckle SAR images and special treatments are needed. Therefore, de-speckle has to be performed to present high resolution SAR images for remote sensing analysis [1].

Several algorithms were presented in literature to remove speckle noise from SAR images. These techniques are of two categories, One is multi look processing, which is an incoherent addition of independent images of same scene. But this leads to degradation of image resolution due to multiple scans of the terrain. Second category is filtering. The Kuan [2],Lee[3] and median filters are typical examples of such techniques. These adaptive low

ISSN: 1992-8645 www.jatit.org E-ISSN: 1817-3195

pass filtering techniques are simple and efficient, but are not able to preserve the image sharpness, also their performance is depends on the terrain of interest. Apart of these, discrete wavelet transform(DWT) is also a technique to suppress speckle noise from radar images. But in DWT processing, due to transforming the image into sub bands some of the important coefficient may miss. In order to avoid this, another wavelet called non-decimated wavelet transformation (NDWT) applied on SAR images to suppress speckle component. The key operation of NDWT is to fill the gaps caused by decimation step in DWT. Thus NDWT leads to redundant and over determined representation of original data. However, in any such techniques selecting the threshold is an important task. Several thresholding techniques were presented in literature such as, soft, hard, sure shrink, oracle shrink, bayes shrink, neural network thresholding etc. Brute force thresholding (BFT) performs better than these thresholding techniques [4]. By considering the limitations of various techniques we propose BFT based speckle suppression to obtain high resolution SAR images. The proposed method is a hybrid technique based on directional smoothing and BFT to de-speckle the radar image. This treatment is well suited for analyzing EM images in real time remote sensing applications.

The next stage in SAR image analysis is enhancement process. In SAR applications, enhancement of radar image is required for extracting precise information from the edges. The edge information gets degraded during de-speckling process. The familiar edge preserving decomposition techniques are of two types. One is local filter based technique, such as bilateral filtering (BLF). Basically BLF is an accelerated version of variants of median filters [5]-[8] and its iterative versions [9], guided image filter (GIF) [10]. The second type is global optimization based algorithms such as total variants (TV) [11], weighted least squares (WLS) [12] and its improved versions like fast weighted least squares (FWLS) [13]and L_0 norm gradient minimization [14]. Hence edge preserving smoothing is required for SAR analysis. By subtracting the smoothened image from the input image, a detailed layer of the input image is obtained. So edge preserving and smoothing algorithms could be used for SAR enhancement process. Global optimized filters perform better in enhancement process. Another technique for enhancement is texture removal. Bilateral texture filter [16] is one of such technique proposed recently. For better performance guidance filter and BLF are combined by invoking BLF in the iterations. By doing so, texture from the image could be removed. BLF [4] process the images by combining domain filter and range filter for preserving edges. It is simply widely used weighted average filter but it suffers from the gradient reversal artifacts. GIF is one of the fastest edge preserving filter it computes the resulting image by considering the structure of guidance image. Nevertheless, this model cannot represent the images well near edges [10]. The halos at the edges produce the poor visual quality at the edges and thus it is the main problem of GIF. WGIF is able to reduce these halo artifacts of GIF and preserve the edge effectively. In both GIF and WGIF first order constraints are specified for smoothing. There are no explicit constraints to treat the edge in both algorithms. Based on these arguments it is needed to develop a new technique which is able to treat edges efficiently. Hence, to meet these requirements a gradient domain guided filter is proposed for edge preserving based on local optimization and cost function. This is composed of first order regularization term and zeroth order fidelity term. Therefore, the proposed image conditioning process consists of two stages. One is de-speckle process based on directional smoothing and brute force thresholding. The second stage is image enhancement process based on a gradient domain GIF (GDGIF). The theory and experiments performed on these methods are presented in the next sections.

2. SAR IMAGE DENOISING AND ENHANCEMENT

The process of denoising and enhancement of a SAR image is the major task to analyze the terrain features. These two operations are considered as preprocessing and post processing of the image. In preprocessing we apply techniques to remove speckle noise from the radar image, whereas during post processing we apply enhancement techniques to enable the image for terrain feature identification.

2.1. Preprocessing

Speckle reduction is an important preprocessing technique in any synthetic aperture based imaging radar. The basic source of speckle noise is the random interference between the coherent returns from the numerous scatters appeared on the terrain along the length of synthetic aperture. In SAR images the widely used techniques to suppress

ISSN: 1992-8645 www.jatit.org E-ISSN: 1817-3195

speckle component are Lee, Gaussian, Wiener, median and frost filters.

In de-speckle process selection of optimum threshold is an important task. Large threshold leads to loss of coefficients that carry image features, whereas small threshold causes retaining the noisy coefficients. Normally, soft thresholding and hard thresholding techniques are used for de-noising applications. Hard thresholding is a keep or kill rule whereas soft thresholding shrinks the coefficients above the threshold in absolute value. It is a shrink or kill rule. These conventional techniques cause poor resolution in SAR applications. Hence, in order to preserve the tiny features of the SAR image during preprocessing in this paper we propose a hybrid de-speckle method based on directional smoothing and brute force thresholding using un-decimated wavelet transforms.

2.1.1. Directional smoothing

During the de-speckling process edges are blurred in a radar image. Hence an image conditioning technique called edge smoothing is required to protect the edges. The following is the step by step procedure carried in edge smoothing using directional smoothing technique [27]. For convenience, we select three masks of size 3x3,5x5 and 7x7.

- In each direction take the average of pixels and stored in array V
  $V(p) = 1/N \sum_i \sum_j Im(n-i, m-j)$ (1)
- Find the value of $V1(p)$ using
  $V1(p) = abs(V(p) - x(r,c))$
  Where, $x(r,c)$ represents the center pixel of the mask.
- Replace the pixel value of x(r,c) by $V(Index)$
  Where $Index=min(V1)$.
  Repeat this procedure for whole image scanned by mask2

2.1.2 Brute force thresholding

BFT provides an optimum threshold to eliminate speckle noise in SAR images. The step by step procedure is presented here.

- Input the wavelet sub bands. Find the minimum and maximum values of wavelet coefficients.
- Execute the loop while threshold is equal to minimum to maximum
- Select the threshold when loop is completed for the best result.

At every decomposition, the radar image is decomposed into wavelet sub bands LL,LH,HL and HH. The next level is applied to low frequency approximation sub bands. Denoising of image is done with the detail wavelet sub bands like horizontal, vertical and diagonal. Throughout the loop maximum and minimum, values of sub band coefficients are calculated and it is stored at the end. Sub band coefficients are considered as threshold value. At the end of the loop optimum threshold value is elevated for best result. The proposed implementation is based on the frame work presented in [20].

The algorithm steps are as follows:

- Let A be the original speckled noisy SAR image. Let B be the total variation filtered image of A. Let C be the filtered image of median filter.
- Using undecimated wavelet transform decompose the image A,B and C into $Sb_{k,A}^{(\epsilon)}$, $Sb_{k,B}^{(\epsilon)}$ and $Sb_{k,C}^{(\epsilon)}$ sub bands. Here k is the decomposition level and ϵ denotes the sub band details such as horizontal, vertical and diagonal information respectively. It is enough to decompose up to the level 3.
- Each level of detail image can be processed using fallowing steps
  i. At each level find the maximum and minimum value of coefficients of sub-bands.
  ii. Iterate the loop for at each level of image while threshold becomes minimum to maximum.
  iii. Determine each pixel of $Sb_{k,A}^{(\epsilon)}$ is low or high based on the threshold value.
  iv. If the pixel is at low level replace the value of the pixels of $Sb_{k,A}^{(\epsilon)}$ with the corresponding value of $Sb_{k,C}^{(\epsilon)}$.
  v. Direction dependent mask is used to determine the edges of the pixels. If the dark portion of the window or mask contains at least on high pixel, then keep the original value of pixel otherwise replace the value with pixel of $Sb_{k,A}^{(\epsilon)}$.
  vi. Apply directional smoothing to each level sub band of $Sb_{k,A}^{(\epsilon)}$.

ISSN: 1992-8645 www.jatit.org E-ISSN: 1817-3195

vii. Again reconstruct the sub-band of image $Sb_{k,A}^{(\epsilon)}$ by inverse undecimated wavelet transform.
viii. Return the step *ii* until complete the iteration and select the threshold value that gives the best result.
ix. Resulted de-noised image should be stored. Let it be *X*.

Therefore, by combining directional smoothing and BFT we propose a hybrid de-speckle technique for SAR images. This technique assures edge preserving and optimum thresholding.

The flow diagram for entire preprocessing is shown in Figure 1.

Journal of Theoretical and Applied Information Technology
15th November 2016. Vol.93. No.1

ISSN: 1992-8645 www.jatit.org E-ISSN: 1817-3195

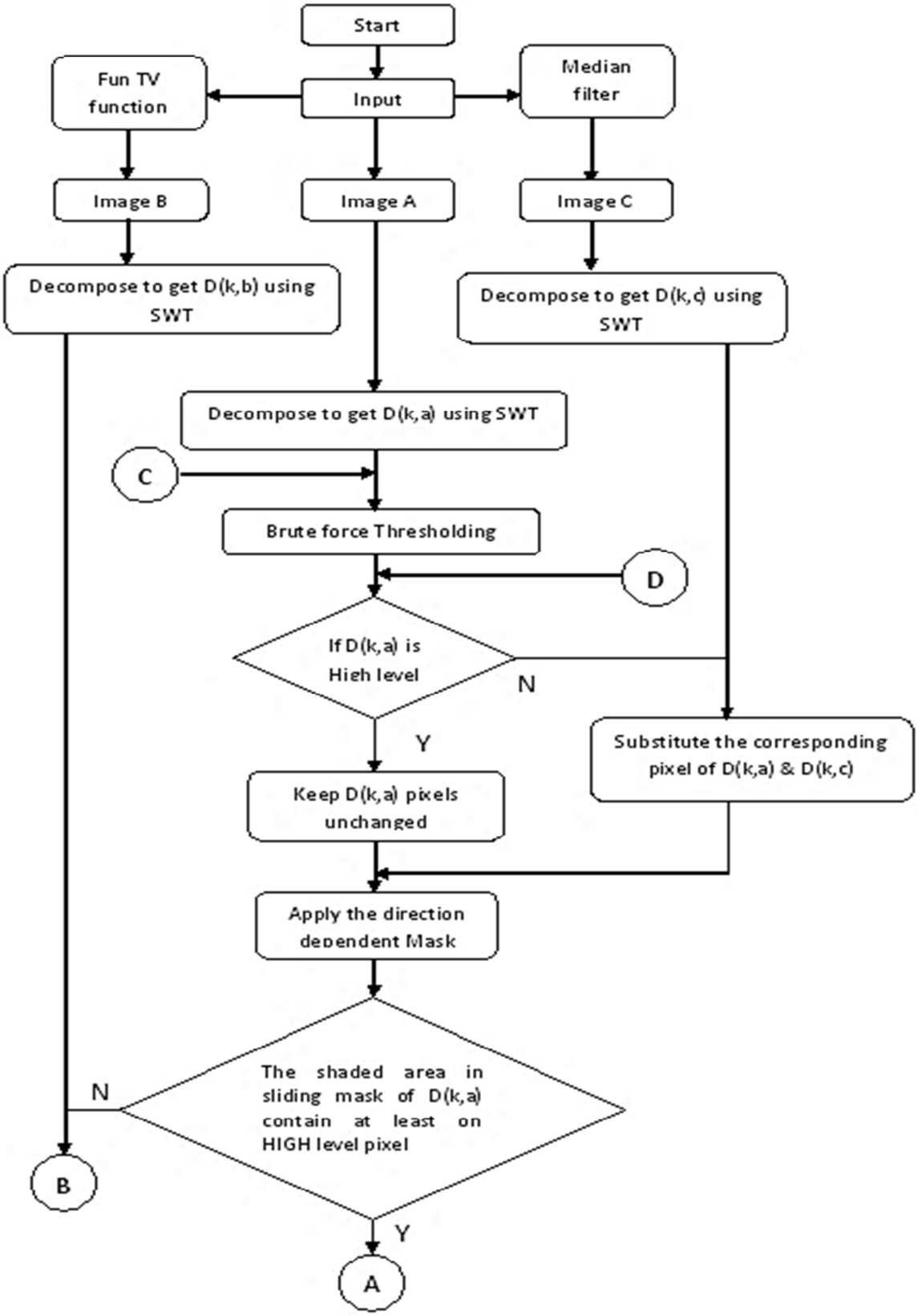

Journal of Theoretical and Applied Information Technology
15th November 2016. Vol.93. No.1

ISSN: 1992-8645 www.jatit.org E-ISSN: 1817-3195

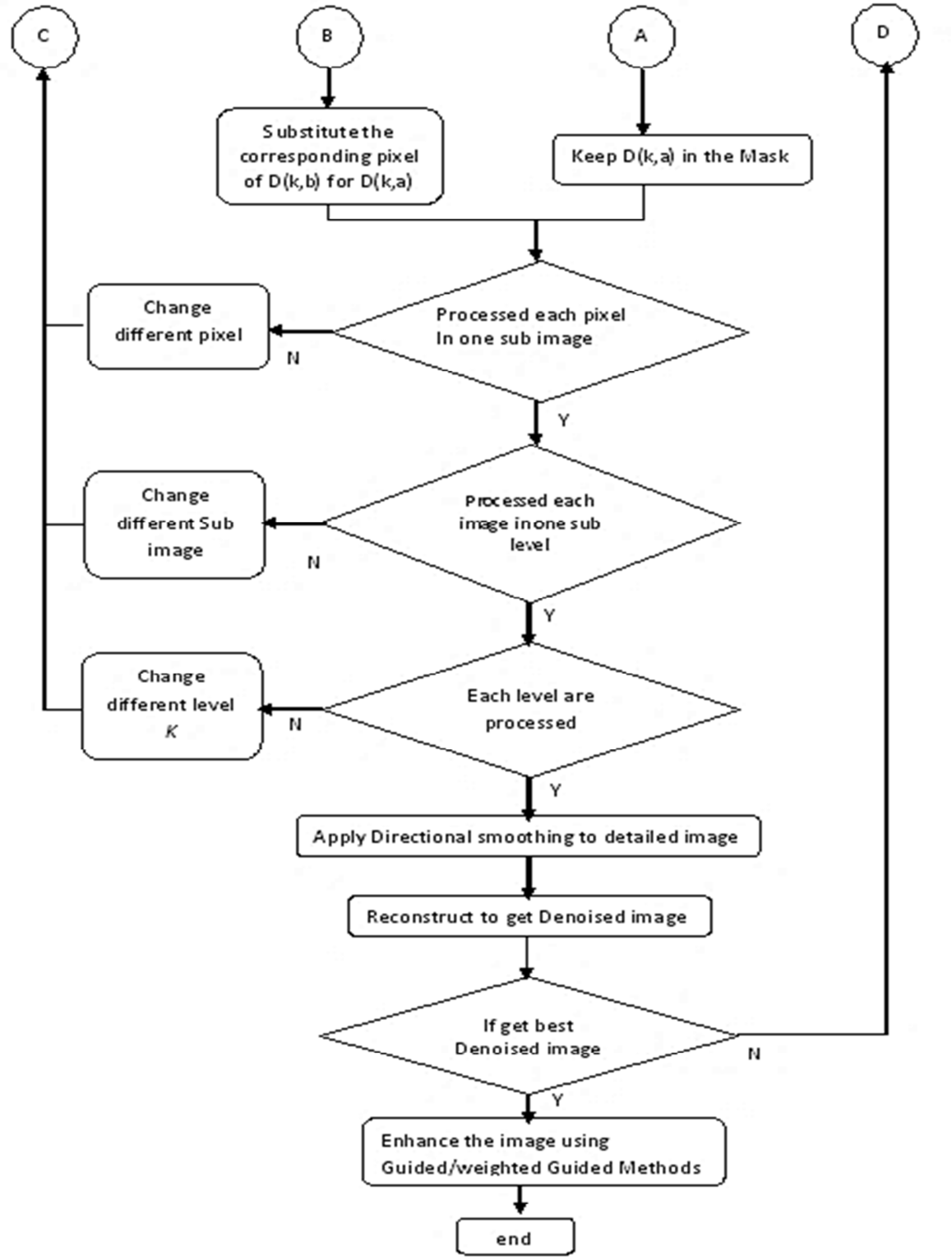

Figure 1.FlowChart of the Proposed Image Conditioning Technique for SAR Image.

Journal of Theoretical and Applied Information Technology
15th November 2016. Vol.93. No.1

ISSN: 1992-8645 www.jatit.org E-ISSN: 1817-3195

2.2. Post-processing

This is the second stage in the proposed image conditioning process. This stage performs SAR image enhancement by preserving the edges without loss of information. The technique is based on local optimization and cost function is composed of first order regularization term and zeroth order fidelity term. This regularization term is different from regularization term in GIF and WGIF [10],[17]. As a result the parameters in the new local linear model can represent at the edges in a better manner. Hence, the resolution of the image increases. The complexity of the proposed filter *O(N)* is same as that of GIF and WGIF.

2.2.1. Background theory related to GIF

In the Guided image filtering (GIF), let X be the image to be filtered and G be the guidance image. Both these images could be identical. Let $\Omega_r(p)$ be the centered window at a pixel *p*, radius *r*and $\dot{Z}$ is the out put image which is linear transform of the guidance image G in the window$\Omega_r(p')$ [18], [19].

$$\dot{Z}(p) = C1_{p'}G(p) + C2_{p'} \forall p \in \Omega_r(p') \quad (2)$$

Where C1 and C2 are the coefficients of the window. Their values should be obtained by minimizing the cost function *E(C1,C2)* which represented as

$$E = \sum_{p=\epsilon\Omega_r(p')}[\big(C1G(p) + C2 - X(p)\big)^2 + \lambda C1^2] \quad (3)$$

Where λ is regularized parameter penalizing large *C1*.The optimum values of C1 and C2 are computed as

$$C1 = \mu_{G\odot X,r}(p') - \mu_{G,r}(p')\mu_{X,r}(p') \quad (4)$$

$$C2 = \mu_{X,r}(p') - C1\mu_{G,r}(p') \quad (5)$$

Where $\odot$ represents the element wise production. $\mu_{G\odot X,r}(p')$,$\mu_{X,r}(p')$ *and* $\mu_{G,r}(p')$ are the mean values of $\odot X$,X and G in the window $\Omega_r(p')$ respectively.

From the previous studies, it is clear that GIF is one of the fastest edge preserving filter which avoids the gradient reversal artifacts. However the λ value is fixed. The major drawback of GIF processing is, the halos are un-avoidable when the GIF is forced to get smooth edges. For this a content adaptive GIF was proposed to overcome this problem. In adaptive GIF the cost function is modified as,

$$E = \sum_{p=\epsilon\Omega_r(p')}[\big(C1G(p) + C2 - X(p)\big)^2 + \frac{\lambda C1^2}{£_G(p')}] \quad (6)$$

Where £ represents the edge weighting factor and it is defined by local variances of the windows of all pixels as

$$£_G(p') = \frac{1}{N}\sum_{p=1}^{N}\frac{\sigma_G^2(p')+\varepsilon}{\sigma_G^2(p)+\varepsilon} \quad (7)$$

$Where\ \sigma_G^2(p')$is variance of image G in window $\Omega_r(p')$ and ε is the small positive constant and its value is estimated as $(0.001X\ L^2)$. Here L represents the dynamic range of input image. In the guidance image all the pixels are used to compute $£_G(p')$. This factor measures the importance of pixel *p'* with respect to whole image. The complexity of $£_G(p')$ is O(N) for image contains N pixels due to the box filter[10].

The optimum values for C1 and C2 are calculated as,

$$C1 = \frac{\mu_{G\odot X,r}(p') - \mu_{G,r}(p')\mu_{X,r}(p')}{\sigma_{G,r}^2(p') + \frac{\lambda}{£_G(p')}} \quad (8)$$

$$C2 = \mu_{X,r}(p') - C1\mu_{G,r}(p') \quad (9)$$

The WGIF [17] takes the role to eliminate the halo artifacts. However both WGIF and GIF specify the zero order constraints to get the pixel values and gradient domain constraints (first order constraints) to smooth the pixel values over time and space. In both the methods there are no explicit constraints to treat the edges. Hence edges may be smooth inevitably when image filtering and edge preserving are considered together. As a result edge preserve is not good in GIF and WGIF based techniques. For this purpose we introduce a novel Gradient Domain GIF (GDGIF) which includes the explicit first order edge aware constraints. It seems to be an integrated version of WGIF.

2.2.2. Gradient domain guided image filter (GDGIF)

The proposed GDGIF follows the linear model i.e., $\nabla\dot{Z}(p) = C1\nabla G(p)$. Here the smooth end of image $\dot{Z}(p)$depends on the value of C1. The edge is well preserved when the C1 value is 1. If the value becomes 0 it is well flat represent the

ISSN: 1992-8645 www.jatit.org E-ISSN: 1817-3195

smoothed. Based on this a new cost function is derived as

$$E = \sum_{p=\epsilon\Omega_r(p')}[\left(C1G(p) + C2 - X(p)\right)^2 + \frac{\lambda(C1-\gamma_{p\prime})^2}{\pounds_G(p')}] \quad (10)$$

Where $\gamma_{p\prime} = 1 - \frac{1}{1+e^{\eta(\zeta(p')-\mu_{\zeta,\infty})}}$

$\mu_{\zeta,\infty}$ is mean value of $\zeta(p')$ is the value of $\sigma_{G,1}(p')\sigma_{G,r}(p')$. η ismeasured from $4/(\mu_{\zeta,\infty} - \min(\zeta(p)))$. It is nothing that the value $\gamma_{p\prime}$ reaches 1 if the pixel p' is at the edge and 0 if it is smooth region. In another way the value of C1 is reaches to 1 if the pixel p' is approaches to 1 and it becomes 0 if it is in smooth region. This clears that the proposed method is less sensitive toλ. So the edges are preserved by GDGIF by than GIF and WGIF.

The optimum solutions are

$$C1 = \frac{\mu_{G\odot X,r}(p') - \mu_{G,r}(p')\mu_{X,r}(p') + \frac{\lambda}{\pounds_G(p')}}{\sigma^2_{G,r}(p') + \frac{\lambda}{\pounds_G(p')}} \quad (11)$$

$$C2 = \mu_{X,r}(p') - C1\mu_{G,r}(p') \quad (12)$$

The final value of $\dot{Z}(p) = \overline{C1}G(p) + \overline{C2}$ (13)

Where $\overline{C1}$ and $\overline{C2}$ are the mean values of C1 and C2 in the window respectively.

For easy analysis the images G and X are assumed to be same.

In GDGIF analysis two cases are needed to be considered.

1. Let the pixel p' is at the edge. The value of $\gamma_{p\prime}$ is generally 1. Then the value of C1 is computed as

$$C1 = \frac{\sigma^2_{G,r}(p') + \frac{\lambda}{\pounds_G(p')}}{\sigma^2_{G,r}(p') + \frac{\lambda}{\pounds_G(p')}} = 1$$

   Whatever be the value of λ, the value of C1 reaches to 1.This indicates that GDGIF preserves the sharp edges more effectively.

2. Let the pixel is flat area the value of $\gamma_{p\prime}$ is generally 0 and the value of $\pounds_G(p')$is usually 1. Then the value of C1 is computed as,

$$C1 = \frac{\sigma^2_{G,r}(p')}{\sigma^2_{G,r}(p') + \frac{\lambda}{\pounds_G(p')}}$$

Here regard less the choice of λ the value of pixel C1 is 1. If the pixel is at the edge, λ value is selected comparable to GIF and WGIF. Obviously the value of C1 becomes 0 if the pixel at the flat area.

3. RESULTS AND DISCUSSION

To prove the ability of the proposed techniques we performed several simulations experiments. Several C-band SAR images of ERS and L-band SAR images of Japanese ALOS are considered to carry out the experiments. The developed techniques are applied on these images and performance measures are calculated. Simulation results related to both the stages of image conditioning process are discussed individually.

3.1. Discussion on De-speckling Using Proposed Technique

Our proposed treatment is based on directional smoothing and brute force thresholding to remove speckle noise from the SAR images. We carried this experiment on number of images like lena, pepper and boat. In these experiments we added speckle noise and performed de-speckle.

The performance measures are measured and confirmed the effectiveness of the proposed technique. Then, we considered SAR images and applied the de-speckle technique. For our simulation studies we considered single look ALOS L-band SAR image of mountain to hills transition areas with some roads and urban features. For effective presentation we use 1024x1024 images. The performance of the proposed method is compared with BFT based wavelet filter, frost filter, lee filter, median filter, wiener filter and Gaussian filter. The performance measures considered for the evaluation of various techniques are absolute difference (AD), maximum difference (MD), mean square error (MSE), normalized absolute error (NAE), normalized cross correlation (NCC), peak signal to noise ratio (PSNR) and structural content (SC). The mathematical expressions for these parameters are tabulated in Table I. For these parameters calculation we considered different window sizes 3x3, 5x5 and 7x7.

Journal of Theoretical and Applied Information Technology
15th November 2016. Vol.93. No.1

ISSN: 1992-8645 www.jatit.org E-ISSN: 1817-3195

Table 1: Performance Measures in SAR Image Conditioning

Measure	Mathematical Expression
AD	$AD=\sum_{i=1}^{P}\sum_{j=1}^{Q}((I(i,j)-I'(i,j))/PQ$
MD	$MD= Max(\|(I(i,j)-I'(i,j)\|$
MSE	$MSE=\frac{1}{PQ}\sum_{i=1}^{P}\sum_{j=1}^{Q}(I(i,j)-I'(i,j))^2$
NAE	$NAE=\sum_{i=1}^{P}\sum_{j=1}^{Q}\|(I(i,j)-I'(i,j)\|/ \sum_{i=1}^{P}\sum_{j=1}^{Q}\|(I(i,j)\|$
NCC	$NCC=\sum_{i=1}^{P}\sum_{j=1}^{Q}(I(i,j)I'(i,j)/ \sum_{i=1}^{P}\sum_{j=1}^{Q}I(i,j)^2$
PSNR	$PSNR= 10log\ 255^2/MSE$
SC	$SC=\sum_{i=1}^{P}\sum_{j=1}^{Q}I(i,j)^2/\sum_{i=1}^{P}\sum_{j=1}^{Q}I'(i,j)^2$

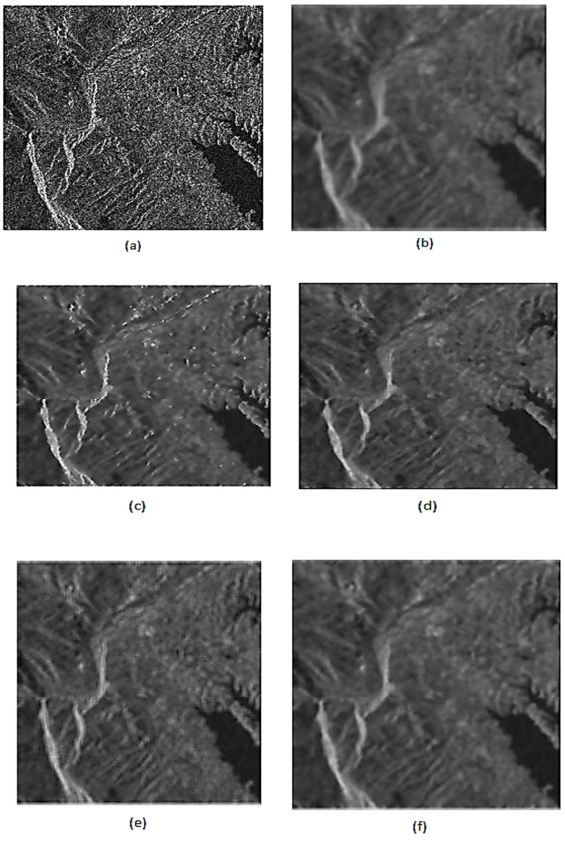

Figure 2. De-speckling results of SAR image. The filters used in (c) - (f) are 5x5. (a). Noisy image (b). Gaussian filter at fc=20, (C). Wiener, (d). Median, (e). Lee, (f). Frost.

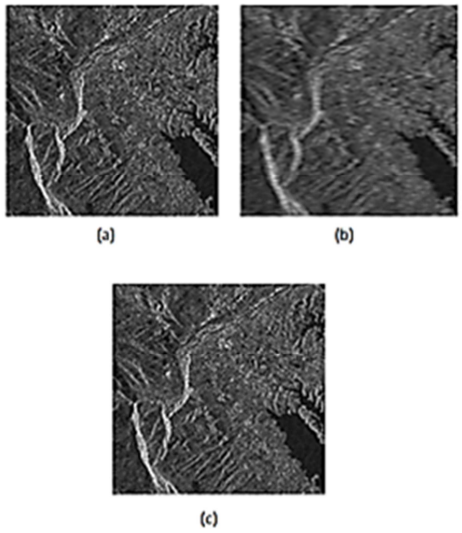

Figure 3. Brute force threshold based wavelet based de-noised results, (a). Adaptive median filtered image, (b). Savitzky-Golay filtered image, (c).De-noised image.

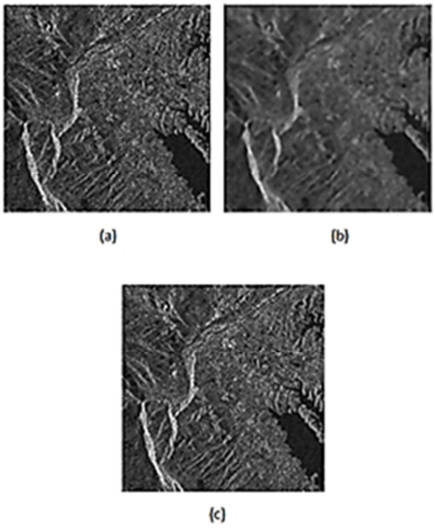

Figure 4. De-speckling results of the proposed method, (a). Total variation function, (b). Median filtered image, (c.) Final de-noised image.

The proposed method is an improved version of BFT based wavelet transform. Fig. 2 shows the de-speckle results of conventional filters like Gaussian, wiener, median and frost filter.

ISSN: 1992-8645 www.jatit.org E-ISSN: 1817-3195

The de-speckle results of adaptive median filter, Savitzky-Golay filter and the de-noised image using proposed method are shown in Fig. 3. Fig. 4 shows the de-speckled image after filtering with the proposed directional finding based technique. The effectiveness of de-speckling by edge preservation particularly identified in the road junction and its urban area in the upper middle part of image. The performance measures computed during de-speckling experiments using various techniques are tabulated in Table I. From these simulation results, it is clear that the proposed directional smoothing based BFT technique performs better than the other counter parts in de-speckling experiments.

Table 2: Performance Metrics For Different De-Noising Filters

Filter type	Level / Window size/ Freq.	Performance Metrics						
		AD	MD	MSE	NAE	NCC	PSNR	SC
Proposed FilterP1	Level 1	-1.4E-16	0.210	2.72E-04	0.021	0.997	35.658	1.004
Proposed FilterP2	Level 2	1.1E-05	0.268	3.78E-04	0.024	0.997	34.220	1.005
Proposed FilterP3	Level 3	-6.8E-08	0.261	4.1E-04	0.025	0.997	33.92	1.005
Brute Force thresholdBased wavelet FilterBFT3	3x3	2.5E-05	0.311	0.001	0.033	0.995	31.615	1.008
Brute Force thresholdbased wavelet FilterBFT5	5x5	2.8E-05	0.334	0.001	0.039	0.993	30.333	1.011
Brute Force thresholdbased wavelet FilterBFT7	7x7	2.9E-05	0.333	0.001	0.043	0.992	29.657	1.013
Frost Filter F3	3x3	2.3E-04	0.366	0.006	0.124	0.974	22.518	1.032
Frost Filter F5	5x5	4.4E-04	0.465	0.007	0.139	0.968	21.510	1.040
Frost Filter F7	7x7	7.3E-04	0.493	0.008	0.147	0.963	20.978	1.047
Lee Filter L3	3x3	2.8E-03	114	363.72	0.123	0.977	22.523	1.030
Lee Filter L5	5x5	1.4E-03	131	473.12	0.140	0.969	21.381	1.040
Lee Filter L7	7x7	1.1E-03	130	556.82	0.151	0.963	20.674	1.050
Median Filter M3	3x3	1.6E+00	191	458.44	0.132	0.963	21.518	1.050
Median Filter M5	5x5	1.6E+00	191	458.44	0.132	0.963	21.518	1.050
Median Filter M7	7x7	1.6E+00	191	458.44	0.132	0.963	21.518	1.050
Wiener Filter W3	3x3	2.8E-02	60	251.04	0.103	0.982	24.133	1.020
Wiener Filter W5	5x5	1.6E-01	73	333.35	0.119	0.976	22.902	1.030
Wiener Filter W7	7x7	3.5E-01	90	379.99	0.127	0.971	22.333	1.040
Gaussian Filter G1	fc=10	1.2E+00	153	779.35	0.176	0.936	19.214	1.090
Gaussian Filter G2	fc=20	3.1E-01	133	528.88	0.147	0.960	20.897	1.050
Gaussian Filter G3	fc=30	1.4E-01	115	419.09	0.132	0.969	21.908	1.040
Optimum Values obtained in these experiments		-6.8E-08	0.210	2.72E-04	0.021	0.963	35.658	1.004

3.2. Discussion on enhancement using proposed technique

Here an L band SAR image is considered to study the enhancement performed by proposed gradient domain GIF. Fig. 5 shows the enhancement results of proposed GDGIF and its counter parts. From this enhancement experiment it is clear that the edge preserving and smoothing capabilities of GDGIF is better than other

ISSN: 1992-8645 www.jatit.org E-ISSN: 1817-3195

techniques. This is illustrated in Fig 5. (a)-(c), the zoomed patches are shown in Fig 5. (d)-(f). The key factor in GIF and *Lo* norm minimization is λ. In GDGIF, λ value is bigger than the other methods. This increased λ value produce larger artifacts in GIF and *Lo* norm minimization than GDGIF. From the zoomed patches shown in Fig 5. (d)-(f) it is clear that the proposed filter has less artifacts than its counter parts.

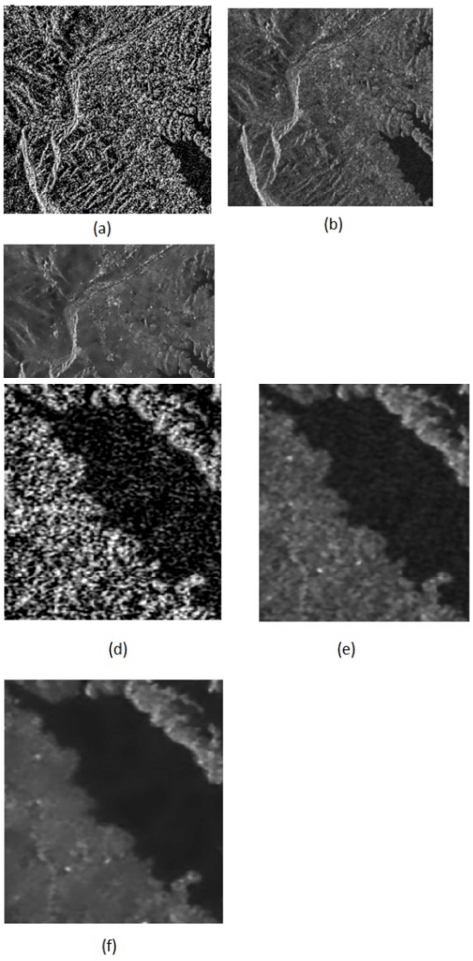

Figure.5. Enhancement results of SAR image. (a). Lo smoothing, (b). Guided Image Filter,(c).Gradient domain GIF, (d).Zoomed patch of Lo smoothing, (e).Zoomed patch of Guided Image Filter, (f).Zoomed patch of GDGIF enhancement.

4. CONCLUSION

In this paper we propose new techniques for the analysis of radar images. In typical imaging radar in order to extract the terrain features and observation some conditioning techniques needed to be applied. In that aspect, in this work we propose novel de-speckle and enhancement techniques for a SAR. The proposed de-speckle technique involves directional smoothing and brute force thresholding. By comparing performance measures shown in Table II, the proposed method achieves better results in terms of minimum MD of 0.210, minimum MSE of 2.72E-04 and maximum PSNR of 35.658. In the enhancement process we propose a gradient domain guide image filter. This enhancement technique assures good edge preserving and smoothing capabilities. This increases the resolution of the image for analysis. Further, in order to track targets and terrain features some sophisticated segmentation techniques for SAR images has to me implemented.

REFERENCES

[1] C. Oliver and S. Quegan, *Understanding Synthetic Aperture Radar Images*. Norwood, MA, USA: Artech House, 1998.

[2]. D. Kuan, A. Sawchuk, T. Strand, and P. Chavel, "Adaptive noise smoothing filter for images with signal-dependent noise," *IEEE Trans. Pattern Anal. Mach. Intell.*, vol. PAMI-7, no. 2, pp. 165–177, Mar. 1985.

[3] J. S. Lee, "Refined filtering of image noise using local statistics," *Comput. Graph. Image Process.*, vol. 15, no. 4, pp. 255–269, Apr. 1981.

[4] R. C. Gonzalez and R. E. Woods, *Digital Image Processing*, 2nd ed. Upper Saddle River, NJ, USA: Prentice-Hall, 2002

[5] C. Tomasi and R. Manduchi, "Bilateral filtering for gray and color images," in *Proc. 6th Int. Conf. Comput. Vis. (ICCV)*, Bombay, India, Jan. 1998, pp. 836–846.

[6]. F. Durand and J. Dorsey, "Fast bilateral filtering for the display of high dynamic-range images," *ACM Trans. Graph.*, vol. 21, no. 3, pp. 257–266, Jul. 2002.

[7]. S. Paris and F. Durand, "A fast approximation of the bilateral filter using a signal processing approach," in *Proc. 9th Eur. Conf. Comput. Vis. (ECCV)*, Graz, Austria, 2006, pp. 568–580.

[8]. F. Porikli, "Constant time *O(1)* bilateral filtering," in *Proc. IEEE Conf. Comput. Vis.*

ISSN: 1992-8645 www.jatit.org E-ISSN: 1817-3195

Pattern Recognit. (CVPR), Anchorage, AK, USA, Jun. 2008, pp. 1–8.

[9]. Q. Zhang, X. Shen, L. Xu, and J. Jia, "Rolling guidance filter," in *Proc13th Eur. Conf. Comput. Vis. (ECCV)*, Zurich, Switzerland, Sep. 2014, pp. 815–830.

[10]. K. He, J. Sun, and X. Tang, "Guided image filtering," *IEEE Trans. Pattern Anal. Mach. Learn.*, vol. 35, no. 6, pp. 1397–1409, Jun. 2013.

[11]. F. Argenti, T. Bianchi, and L. Alparone, "Multi-resolution MAP de-speckling of SAR images based on locally adaptive generalized Gaussian pdf modeling," *IEEE Trans. Image Process.*, vol. 15, no. 11, pp. 3385–3399,Nov. 2006.

[12]. L. Rudin, S. Osher, and E. Fatemi, "Nonlinear total variation based noise removal algorithms," *Phys. D, Nonlinear Phenomena*, vol. 60, no. 1–4,pp. 259–268, Nov. 1992.

[13]. Z. Farbman, R. Fattal, D. Lischinski, and R. Szeliski, "Edge-preserving decompositions for multi-scale tone and detail manipulation," *ACM Trans. Grap.*, vol. 27, no. 3, pp. 249–256, Aug. 2008.

[14] D. Min, S. Choi, J. Lu, B. Ham, K. Sohn, and M. N. Do, "Fast global image smoothing based on weighted least squares," *IEEE Trans. Image Process.*, vol. 23, no. 12, pp. 5638–5653, Dec. 2014.

[15]. L. Xu, C. Lu, Y. Xu, and J. Jia, "Image smoothing via *L*0 gradient minimization," *ACM Trans. Graph.*, vol. 30, no. 6, Dec. 2011, Art. ID 174.

[16]. H. Cho, H. Lee, H. Kang, and S. Lee, "Bilateral texture filtering," *ACM Trans. Graph.*, vol. 33, no. 4, 2014, Art. ID 128.

[17]. Z. Li, J. Zheng, Z. Zhu, W. Yao, and S. Wu, "Weighted guided image filtering," *IEEE Trans. Image Process.*, vol. 24, no. 1, pp. 120–129,Jan. 2015.

[18] A. Torralba and W. T. Freeman, "Properties and applications of shape recipes," in *Proc. IEEE Comput. Vis. Pattern Recognit. (CVPR)*, Jun. 2003, pp. II-383–II-390.

[19] A. Levin, D. Lischinski, and Y. Weiss, "A closed-form solution to natural image matting," *IEEE Trans. Pattern Anal. Mach. Intell.*, vol. 30, no. 2, pp. 228–242, Feb. 2008.

[20]. Yao Zhao, JianGuo Liu," Adaptive Total Variation Regularization Based SAR Image Despeckling and Despeckling Evaluation Index" *IEEE TRANSACTIONS ON GEOSCIENCE AND REMOTE SENSING,* VOL. 53, NO. 5, MAY 2015.

[21]. A. Chambolle, "An algorithm for total variation minimization and applications," J. Math. Imag. Vision, vol. 20, no. 1/2, pp. 89–97, Jan. 2004.

[22].G. Peyre, Total Variation Regularization with Chambolle Algorithm.[Online]. Available: http://www.coe.utah.edu/~0/readings/TotalVariationRegularizationwithChambolleAlgoriht m.pdf.

[23]. M. Hua, X. Bie, M. Zhang, and W. Wang, "Edge-aware gradient domain optimization framework for image filtering by local propagation," in Proc. IEEE Conf. Comput. Vis. Pattern Recognit. (CVPR), Columbus, OH, USA, Jun. 2014, pp. 2838–2845.

[25]. A. Levin, D. Lischinski, and Y. Weiss, "A closed-form solution to natural image matting," IEEE Trans. Pattern Anal. Mach. Intell., vol. 30, no. 2,pp. 228–242, Feb. 2008.

[26]. D. R. Martin, C. C. Fowlkes, and J. Malik, "Learning to detect natural image boundaries using local brightness, color, and texture cues," IEEE Trans. Pattern Anal. Mach. Intell., vol. 26, no. 5, pp. 530–549, May 2004.

[27]. V. Lakshmanan, "A Separable Filter for directional smoothing", IEEE geo sc. and remote sensing letters, vol. 1, pp. 192-195, 2004.